Available online at www.sciencedirect.com
ScienceDirect
Polymer 48 (2007) 3183–3191
polymer
www.elsevier.com/locate/polymer

Effect of fiber reinforcement on the tensile, fracture and thermal properties of syntactic foam

Erwin M. Wouterson [a], Freddy Y.C. Boey [a], Xiao Hu [a], Shing-Chung Wong [b,*]

[a] School of Materials Science and Engineering, Nanyang Technological University, Nanyang Avenue, Singapore 639798, Republic of Singapore
[b] Department of Mechanical Engineering, University of Akron, Akron, OH 44325-3903, USA

Received 27 October 2006; received in revised form 28 March 2007; accepted 29 March 2007
Available online 5 April 2007

Abstract

This paper examines the effect of the fiber content and fiber length on tensile, fracture and thermal properties of syntactic foam. Results showed that a hybrid structure demonstrates a significant increase in the ultimate tensile strength, σ_{uts}, and Young's modulus, E, with increasing fiber loading. Interestingly, the fracture toughness, K_{Ic}, and energy release rate, G_{Ic}, increased by 95% and 90%, respectively, upon introduction of 3 wt% short carbon fibers in syntactic foam, indicating the potent toughening potential for short carbon fibers in syntactic foam systems. SEM and OM studies identified the presence of several toughening mechanisms. An estimate of the contribution from each toughening mechanism by composite theory and fractography revealed that the specific energy required to create new surfaces was enhanced by the presence of fibers and was the main contributor to the toughness of the short fiber reinforced syntactic foam.

Keywords: Syntactic foam; Fiber reinforced polymers; Toughness

1. Introduction

Syntactic foam, which is derived from a mixture of resin (binder) and hollow microspheres (filler), is a special class of light-weight composite materials, the mechanical and fracture properties of which are not well understood [1–3]. In the studies of foam-based materials, most concentrate on foams that require chemical blowing agents [4,5]. The density of the resulting foams cannot be determined a priori. Syntactic foam enables one to pre-determine the density of the composite. Fiber reinforced syntactic foam and other hybrid forms of foams including one containing nanoparticles have received little attention [6,7]. In a series of studies [8,9], we critically examined these novel filler types in syntactic foams and their individual roles in altering the mechanical and fracture properties in the hybrid systems. In this paper, we aim to examine the role of fibers in reinforcement and toughening of syntactic foams. This study is considered novel because an understanding of the fracture mechanics and mechanisms of hybrid syntactic foams is lacking.

Syntactic foam is an attractive core material in sandwich composites because of its low density, high stiffness, excellent compressive and hydrostatic strengths, and low moisture absorption [10]. Recently, we reported the influence of the foam microstructures on the specific mechanical and fracture properties [8]. It was observed that the fracture toughness of syntactic foam came to a maximum near 20–30 vol% microspheres. To enable wider applications for syntactic foam, it is necessary to increase the fracture toughness such that the foam-based materials can be employed in high-impact, damage-tolerant conditions. Fiber toughening, whereby short fibers are dispersed in a polymeric material, is a technique that was used for reinforcement and toughening of engineering plastics [11–13], but it has less been explored for syntactic foams. Generally, short fibers can toughen the polymer matrix via crack deflection and enhanced matrix deformation, and

* Corresponding author. Tel.: +1 330 972 8275; fax: +1 330 972 6027.
E-mail address: swong@uakron.edu (S.-C. Wong).

0032-3861/$ - see front matter © 2007 Elsevier Ltd. All rights reserved.
doi:10.1016/j.polymer.2007.03.069

less so for fiber breakage and fiber pull-out due to the less than effective fiber lengths to induce breakage and optimize pull-out work. A critical advantage for fiber toughening in comparison to rubber toughening is that concomitant increase in toughness and stiffness can be accomplished by short fiber reinforcements.

Little is understood on short fiber reinforced syntactic foam (SFRSF) [6]. This paper aims to evaluate the toughening potential via hybrid structures using SFRSF. Fracture mechanics and microscopic techniques are employed. Thermal and mechanical properties will be examined. The results will be discussed in light of known toughening mechanisms operative in fiber and microsphere reinforced epoxy. The benefits of such an evaluation can lead to wider applications using light-weight structural composites.

2. Experimental work

2.1. Materials and equipment

The syntactic foam for this research was produced by mechanical dispersion of hollow microspheres in epoxy resin. Phenoset BJO-093 hollow phenolic microspheres were used for the filler. The amount of microspheres was fixed at 30 vol% as this reflected the highest fracture toughness of syntactic foam in our previous work [8]. Epicote 1006 epoxy resin was used as the binder. The resin is a combination of liquid bisphenol-A, epichlorohydrin epoxide resin, amine and polymeric additives. Short carbon fibers (SCF) were used as the fiber reinforcement. The SCF were cut by hand from a 0°/90° carbon fiber mat. The fiber is on an average 7 μm in diameter. To study the effect of the fiber length on the tensile and fracture properties, fibers with three different lengths were cut from the 0°/90° carbon fiber mat. The distribution of the fiber lengths was analyzed by measuring the fiber length from a digital image using the public domain software ImageJ [14]. The number average distributions of the fiber lengths are shown in Fig. 1. The mean fiber lengths obtained are 3.11, 4.50, and 10.05 mm.

To study the effect of the fiber weight fraction on the tensile and fracture properties, 1, 2, and 3 wt% SCFs were added to the epoxy resin. The SCF were added to the epoxy resin, followed by microspheres. This mixing order results in a reduction of air bubble present in the curing process. The microspheres were added in multiple steps to the epoxy resin to avoid agglomeration. Previously, we observed that for pristine syntactic foam the microspheres showed a tendency to float on the top surface due to their low density compared to the binder [8]. This effect was minimal for SFRSF due to the increased viscosity of the mixture and by stirring the mixture close to the gel time, which was about 60 min, for the epoxy. Scanning electron micrographs confirmed the homogeneity of the SFRSF. After dispersion, the SFRSF was compression molded using an aluminum mold coated with a silicone release agent. The mixture was left under the press at a pressure of 1.6 MPa for 18–22 h to cure at room temperature.

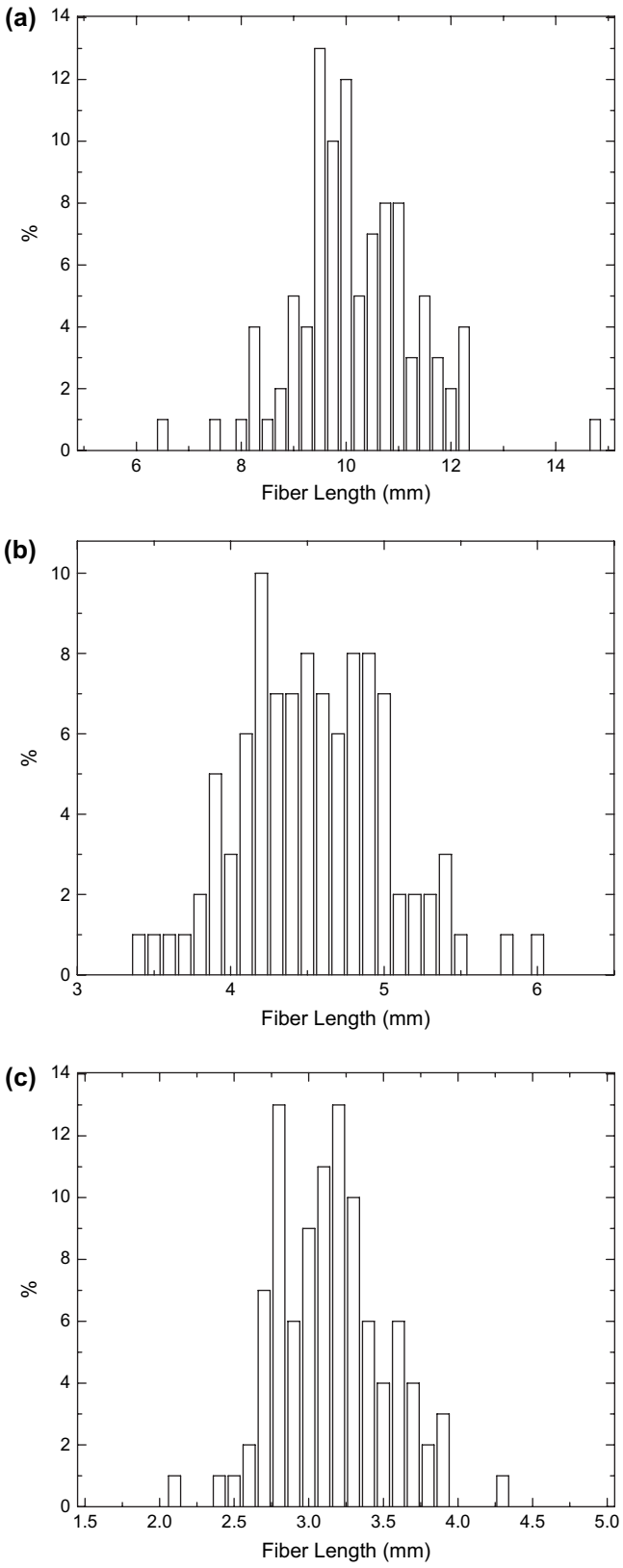

Fig. 1. Distributions of three different average fiber lengths chosen: (a) 3.11, (b) 4.50 and (c) 10 mm. These fiber lengths are used to examine the effect of fiber lengths on the properties of composites.

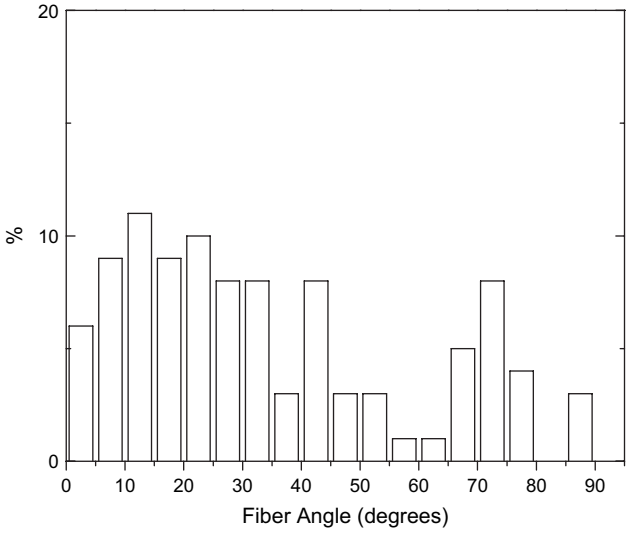

Fig. 2. Fiber angle distribution of the fiber distributions in Fig. 1.

Due to hand mixing, the short fibers are randomly dispersed. The distribution of the fiber angles was obtained using the method presented by Norman and Robertson [15]. The fiber angle distribution was measured from optical micrographs of polished sections using ImageJ [14] available on the public domain on digitized images. Planar fiber angle distributions for the nonaligned specimens are shown in Fig. 2. The planar fiber angle distributions were converted to 3D by assuming the distributions to be symmetric about the field axis. Fig. 3 shows the general microstructures of SFRSF.

2.2. Tensile test

SFRSF was machined into standard 'dog-bone' specimens by means of a TensilKut I from Tensilkut Engineering. The specimens were uniaxially loaded at the ambient temperature using an Instron Model 5567 at a crosshead speed of 5 mm/min. For each test the tensile strain was recorded with a clip-on strain gauge. The Young's modulus, E_t, is measured from the initial elastic region of the stress–strain curve. The results are based on an average of four tests. The error bars represent the standard deviation for four measured values.

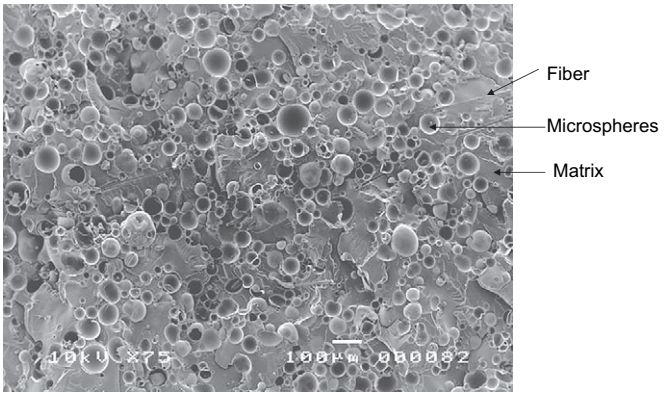

Fig. 3. General microstructures of short carbon fiber reinforced syntactic foam.

2.3. Thermal properties

A high resolution TGA 2950 Thermogravimetric Analyzer (TGA) equipped with TA thermal analysis software was used to study the thermal stability of SFRSF. The specimens, a few mg in weight, were heated from room temperature to 800 °C at 20 °C/min in a nitrogen environment.

Dynamic mechanical analysis (DMA) was performed using a TA DMA 2980. The SFRSF specimen used were rectangular pieces of $55 \times 15 \times 6$ mm^3. The specimens were tested with three-point-bend (3PB) fixtures from room temperature to 110 °C at 5 °C/min. The frequency was 1 Hz.

2.4. Fracture toughness

Single-edge notched bend (SENB) specimens were loaded in a 3PB geometry for fracture toughness assessments. The tests were performed by an Instron Model 5567 at a crosshead speed of 5 mm/min. The specimen dimensions were $60 \times 12.7 \times 6.35$ mm^3.

For all specimens, a constant crack-to-width ratio, a/W, of 0.5 was prepared by a vertical band saw. A sharp crack was introduced by tapping a fresh razor blade into each notch. The critical stress intensity factor, K_{Ic}, can be estimated from the following equations [16]:

$$K_{Ic} = Y \frac{3PS\sqrt{a}}{2tW^2}, \tag{1}$$

$$Y = 1.93 - 3.07\left(\frac{a}{W}\right) + 14.53\left(\frac{a}{W}\right)^2 - 25.11\left(\frac{a}{W}\right)^3 + 25.80\left(\frac{a}{W}\right)^4, \tag{2}$$

where Y is a geometry correction factor, P the peak load at the onset of crack growth in a linear elastic fracture, t the specimen thickness, W the width of the specimen, S the support span, and a is the crack length.

The critical strain energy release rate, G_{Ic}, was calculated from the stress intensity values using the following relationship [17]:

$$G_{Ic} = \frac{K_{Ic}^2}{E_t}\left(1 - \nu^2\right), \tag{3}$$

where, E_t is the Young's modulus and ν is the Poisson's ratio. It should be noted that Eq. (3) is only applicable to plane strain conditions. The value of ν is assumed to be 0.3 as the precise value of ν was not measured. As indicated in Ref. [16] this assumption is justified as the factor cannot change the major results obtained from G_{Ic} conversion in a significant way. The results presented are an average of five specimens. The error bars represent the standard deviations based on five specimens.

After testing, the fracture surface was cut from the specimen. A layer of gold was sputter coated onto the fracture surface by means of a gold coater (SPI module). The fracture behavior of syntactic foam was then characterized by means

of a Jeol JSM 5410LV, a low vacuum scanning electron microscope (SEM).

An optical microscope (Nikon Eclipse E600 POL) was used to study the sub-surface damage in the process zone of a 3PB specimen. The center section, containing the initiated crack was cut from the SENB specimen using a vertical band saw, followed by encapsulation in epoxy resin. To facilitate the study, the sample was polished through the mid-section using a Struers Rotopol-35 polisher. Grinding and polishing were performed using silicon carbide polishing papers with grade numbers from 320, 500, 800, 1200–4000, followed by diamond paste containing particles of 3 μm and 1 μm in sizes. Thin sections were taken from the specimen's mid-plane, perpendicular to the fracture surface by means of a Buehler Petro-thin Thin Sectioning System. The thin section was observed under a transmission optical microscope (TOM) with bright and polarized light.

3. Results and discussion

3.1. Tensile properties

We focus first on the tensile properties of these complex hybrid systems. SFRSF behaves like a linear elastic material when loaded to failure in tension. All samples show a catastrophic failure across a plane perpendicular to the loading direction. Tensile properties are shown in Fig. 4a and b. It is clear that the SCF improves the tensile strength and stiffness of SFRSF. As shown in Fig. 4a, the ultimate tensile strength, σ_{uts}, increases by 40% with the addition of 3 wt% SCF. The increasing trend is similar for various fiber lengths examined. The trend of σ_{uts} with the fiber content is consistent with the data presented by other investigators for short fiber reinforced polymers [15,18,19]. Nevertheless, the uniqueness of this approach is to understand the interactions among fibers, foam and polymer under deformation. For the Young's modulus, see Fig. 4b, a linear additive trend with the increase in SCF weight fraction is observed. The Young's modulus increases from 1.58 GPa for neat syntactic foam to 3.4 GPa for syntactic foam containing 3 wt% SCF, an increase of 115%. Similar to σ_{uts}, the fiber length variation does not affect the E_t of SFRSF.

It is understood that tensile strength can be influenced by fiber orientation. Compared to unidirectional fiber reinforcement, random orientation of the short fibers is known to result in lower reinforcement effectiveness in fiber reinforced polymeric materials [15,18–20]. From composite mechanics theory, see Eq. (4), it can be seen that only 41% of fiber lengths are effective for discontinuous reinforcement in three dimensional (3D) randomly orientated fibers.

$$\bar{l} = \frac{N\int_0^{\pi/2}\int_0^{\pi/2} l\cos\theta\cos\varphi \mathrm{d}\theta\mathrm{d}\varphi}{N(\pi/2)^2} = 0.41l, \tag{4}$$

where, N is the number of fibers, l the fiber length, θ and φ are the projected angles on the loading axis, x, and x–y plane, respectively, in 3D orientation.

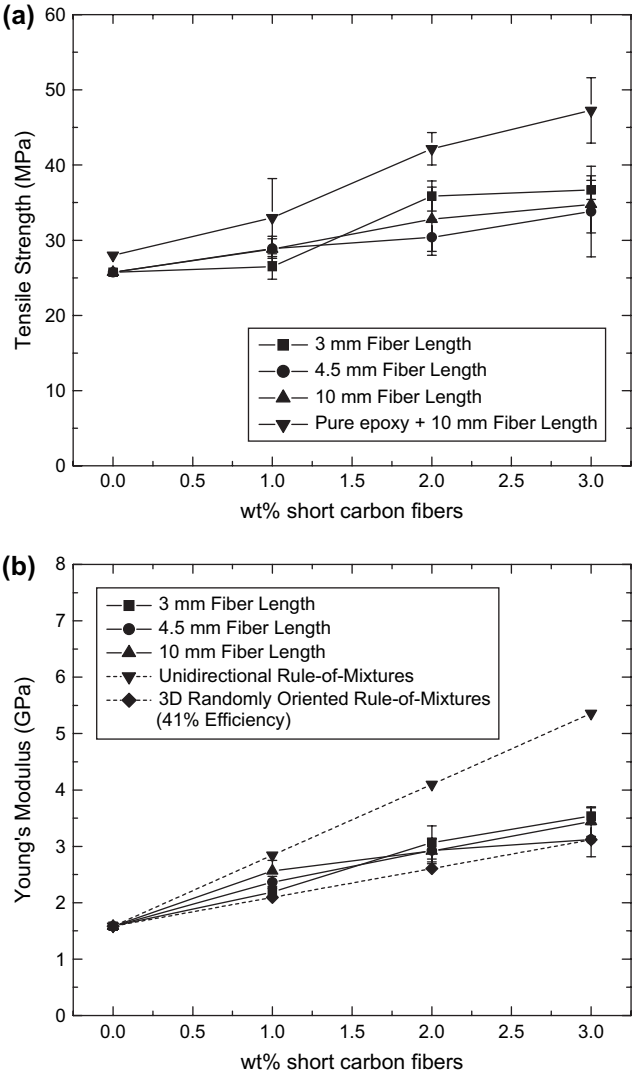

Fig. 4. Tensile properties of short carbon fiber reinforced syntactic foam with different fiber weight fractions and fiber lengths: (a) tensile strength and (b) Young's modulus.

The contrast for reduction in E_t due to random fiber orientation is clearly visible in Fig. 4b. Based on comparison of the slopes of the experimental data, it is determined that SFRSF exhibits an average efficiency of about 48% which is slightly higher than the theoretical 41%. A random fiber orientation of SCFs in the current SFRSF system is expected since the components are mixed by hand in a beaker and poured directly into an open mould.

Fig. 4a and b indicates that the difference in fiber length does not cause a large variation in the tensile properties. With a simple estimation using the Kelly–Tyson model [21], we could demonstrate that the critical fiber transfer length, l_c, is exceeded by the shortest fiber length introduced [22]:

$$l_c = \frac{d\sigma_f}{2\tau_y}, \tag{5}$$

where, σ_f is the fiber strength, d is the fiber diameter, and τ_y is assumed to be the matrix shear strength, which is assumed to

be close to $\tau_y = \sigma_{my}/2$; σ_{my} is the matrix yield strength. Measurements using SEM show that the SCF used for the current research has an average diameter of 7 μm. Based on this diameter, the critical fiber length, l_c, is estimated to be 0.2 mm. Note that Eq. (5) assumes a strong fiber/matrix interface and unidirectional fiber alignment. Fiber end bonding is also ignored. The latter two assumptions do not hold in our current study. However, it could be understood that the current fiber lengths of 3, 4.5, and 10 mm are likely to be compatible if not exceeding l_c.

A detailed analysis of hollow microsphere–fiber interactions is not available in the literature. Based on the contributions of the individual components, the authors believe that the SCF are the main contributor to the tensile strength. Fig. 4a shows that the increase in tensile strength for SCF-reinforced epoxy is significantly higher compared to the increase in SFRSF for similar fiber loadings. The reduced efficiency of SCF in SFRSF could be attributed to a reduced volume fraction of epoxy resin with increasing fiber content. For example, 3 wt% of SCF reduces the volume fraction of syntactic foam by 1.4% and further reduces the volume fraction of epoxy resin in the matrix. The reduction in epoxy resin available may not suffice to wet both the microspheres and fibers, leading to a reduction in the tensile strength. Indeed, a significant increase in the viscosity of pre-cured SFRSF was observed with increasing fiber content suggesting unwetted microspheres and fibers.

3.2. Fractographic examination of the tested tensile specimens

Fractographic examinations of tested tensile specimens, see Fig. 5, show the various toughening mechanisms present in SFRSF. Fractured and debonded fibers, matrix deformation, debonded and crushed microspheres are observed. Fig. 5 also confirms the random orientations of the SCF as both perpendicularly and longitudinally orientated fibers are observed on the fracture surface. Clearly, the matrix around the SCFs shows increased deformation compared to areas without fibers. The fibers are significantly stronger than the microspheres and are likely to bear a higher effective load. Based on simple analysis presented earlier [12], it is estimated that the matrix stress can be reduced by 36–79% by including 1–3 wt% of short glass fibers. It should be noted that the composites analyzed did not contain hollow microspheres. Fig. 4a shows a reduced efficiency of fibers in SFRSF. It is expected that the reduction in the matrix stress will be less in SFRSF.

3.3. Thermal properties

Fig. 6 shows that the thermal stability of SFRSF is independent of the fiber length and fiber weight fractions. For all the samples tested, a substantial weight loss is observed at around 350 °C. The thermal decomposition is completed at 550–600 °C. As the curve for 0 wt% SCF is similar to the ones with SCF content, it can be concluded that the thermal stability of SFRSF is primarily governed by the matrix of the SFRSF.

Fig. 7a and b shows the results from dynamic mechanical analysis (DMA). Fig. 7a shows the effect of the fiber content and fiber length on the storage modulus, E'. Similar to the observation for the uniaxial Young's modulus, the storage modulus increases with the short fiber content. A clear trend with the fiber length is not observed. Despite a slight increase in the glass transition temperature, T_g, compared to neat syntactic foam, it is clear from Fig. 7b that the variations in fiber content and fiber length do not affect the T_g of SFRSF. The peak in the tan δ vs. temperature curve, which is considered to be indicative for T_g, is located at around 69 °C for all samples.

3.4. Fracture toughness

Fig. 8a and b shows the interesting results of the fracture toughness assessment on SFRSF. The most distinctive feature

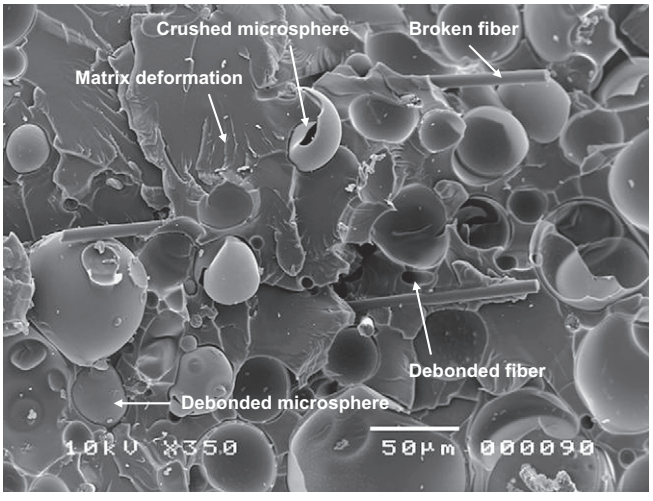

Fig. 5. SEM image of the fracture surface of short carbon fiber reinforced syntactic foam subjected to tensile loading.

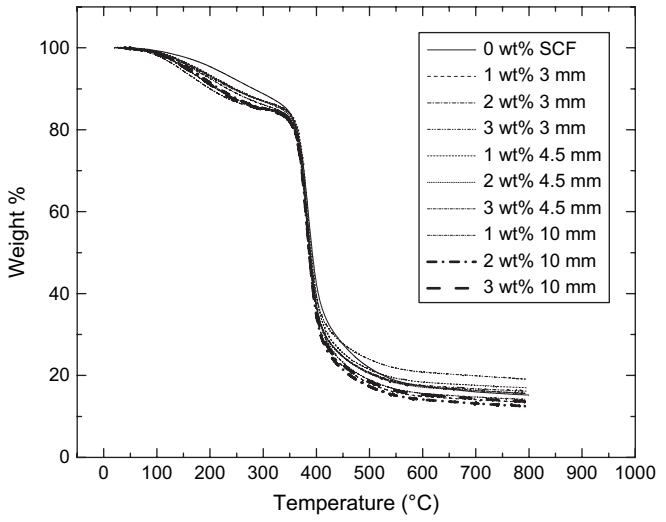

Fig. 6. Weight loss vs. temperature for short carbon fiber reinforced syntactic foam with different fiber weight fractions and fiber lengths.

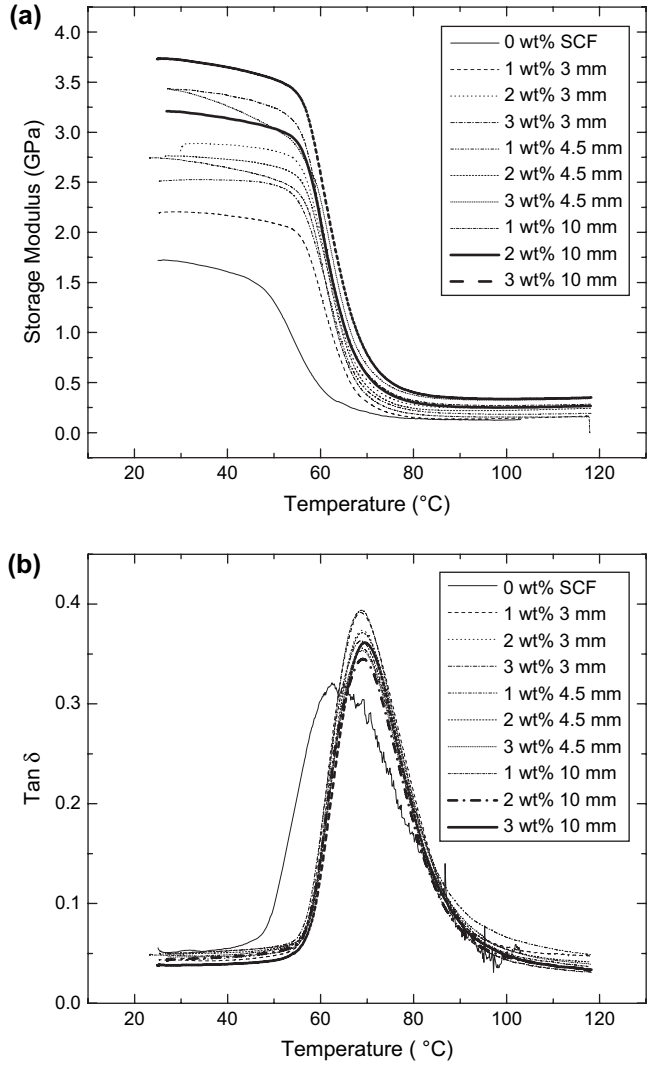

Fig. 7. (a) Storage modulus and (b) tan δ vs. temperature for short carbon fiber reinforced syntactic foam with different fiber weight fractions and fiber lengths.

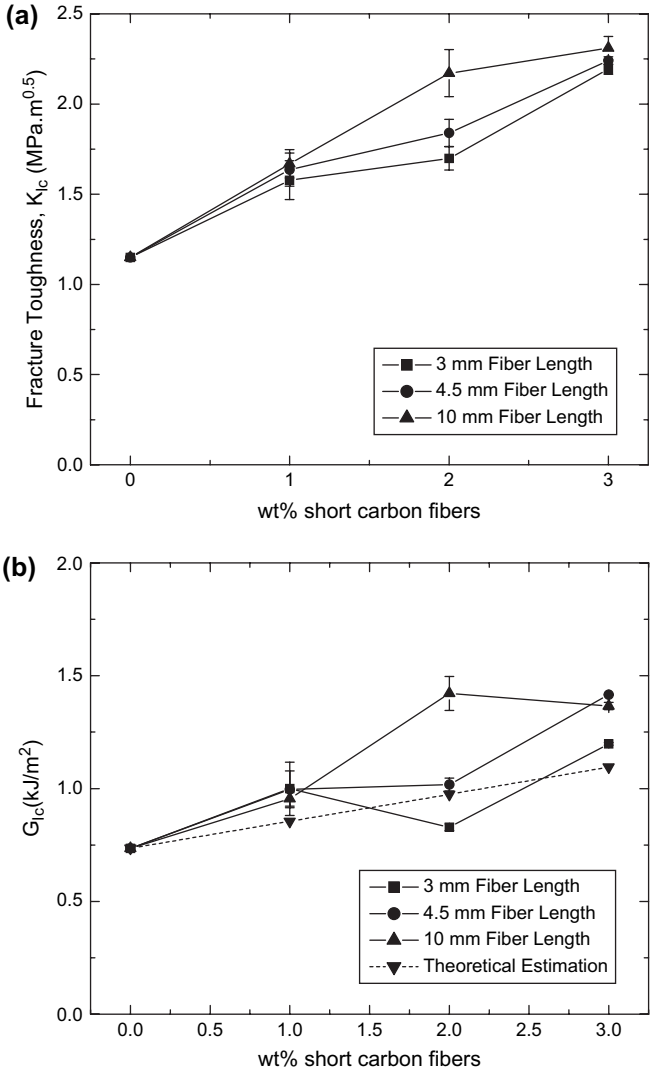

Fig. 8. Effect of fiber content and fiber length on the fracture properties of short carbon fiber reinforced syntactic foam: (a) critical stress intensity factor, K_{Ic} and (b) critical energy release rate, G_{Ic}.

in Fig. 8a is the increase in the plane strain fracture toughness, K_{Ic}, with increasing fiber content. The results suggest the synergistic benefit of fiber reinforcement in syntactic foam. It is evident that concomitant increases in both tensile strength and fracture toughness can be accomplished in a hybrid system of SFRSF. K_{Ic} increases from 1.15 MPa m$^{0.5}$ for neat syntactic foam to 2.25 MPa m$^{0.5}$ for a composition containing 3 wt% fibers, an impressive increase of about 95%. The variation in K_{Ic} values for SFRSF containing 2 wt% of short fibers is attributed to irregular tapping of the sharp crack. Fracture toughness is governed essentially by the local deformation events such as one embedded in a fracture process zone, and is less dependent on the global properties as compared to stiffening mechanisms. Interactions between the reinforcing components including SCF and microsphere, and the epoxy matrix are complex. Thus, a clear explanation of the varying fracture toughness awaits more microscopic evidence.

The critical energy release rate, G_{Ic}, which is calculated from the K_{Ic} and the respective Young's modulus data, are shown in Fig. 8b. Despite the deviation in results for 2 wt% SCF reinforcement, which is mainly caused by the deviation previously observed for K_{Ic}, a general increasing trend in G_{Ic} is observed when the fiber content is increased from 0 to 3 wt%. Increase in both K_{Ic} and G_{Ic} indicates the excellent toughening potential of SCF in syntactic foams.

Optical microscopy (OM) was performed to evaluate the possible presence of micro-shear banding as reported by Lee and Yee [23,24]. Micro-shear banding has been reported as an important toughening mechanism in glass sphere reinforced polymers. An image of the sharp crack and crack initiation region obtained with a transmission optical microscope (TOM) is shown in Fig. 9. The image clearly shows the presence of fiber bridging and debonding of microspheres at the crack interface. Despite observing multiple specimens containing different amounts of reinforcing fibers under the optical microscope, no micro-shear banding can be seen under polarized light.

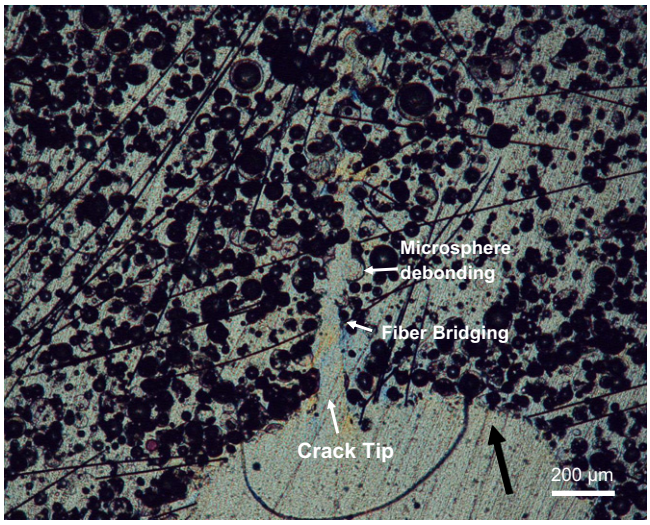

Fig. 9. Transmission optical micrograph showing the sub-surface damage near the sharp and initiation crack area in short carbon fiber reinforced syntactic foam. The black arrow indicates the direction of crack propagation.

An SEM fractograph of an SENB specimen is shown in Fig. 10. Various toughening mechanisms, including fiber pull-out, fiber breakage, step structures [25], debonding of microspheres and fractured microspheres are identified. The presence of multiple toughening mechanisms on the fracture surface of SENB specimens requires an in-depth analysis to determine individual contribution to the overall toughness of the composite. The presence of fiber breakage, interface debonding and pull-out suggests the presence of fiber bridging during the fracture process. Fiber bridging is known to be a major toughening mechanism in fiber reinforced polymer composites. Based on the results presented by Kim and Mai [22], together with the fact that the fiber length is significantly larger than the critical fiber length, we have identified in this study the following contributions affecting the overall fracture toughness of short fiber reinforced syntactic foam:

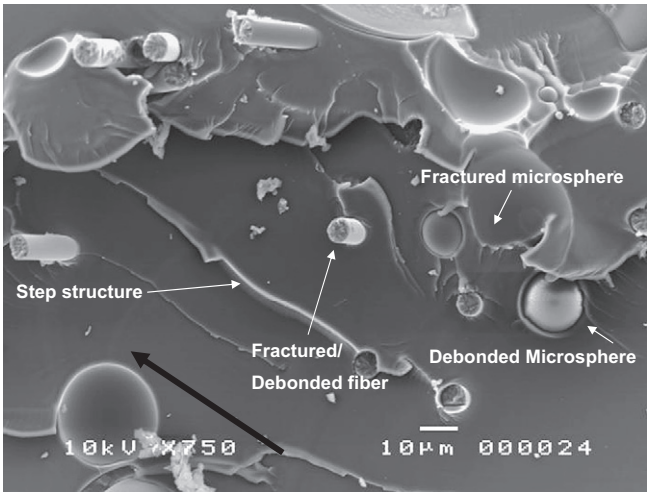

Fig. 10. SEM image of the fracture surface of an SENB specimen of short fiber reinforced syntactic foam. The black arrow indicates the direction of crack propagation.

Interfacial debonding

$$R_d = \frac{V_f \sigma_f^2 l_d}{2E_f}, \tag{6}$$

Redistribution of the strain energy

$$R_r = \frac{V_f \sigma_f^2 l_c}{3E_f}, \tag{7}$$

Fiber pull-out

$$R_{po} = \frac{V_f \tau_{fr} l_c^2}{6d} \frac{l_c}{l}, \tag{8}$$

Formation of new surfaces

$$R_s = \left[V_f \left(\frac{l_c}{d} - 1 \right) + 1 \right] R_{sf}, \tag{9}$$

Total toughness

$$R_t = R_d + R_r + R_{po} + R_s, \tag{10}$$

where V_f is the fiber volume fraction, σ_f the fiber strength, l_d the debonding length, l_c the critical fiber length, E_f the Young's modulus of the fiber, d the fiber diameter, τ_{fr} the frictional shear stress, and R_{sf} is the toughness of the unreinforced syntactic foam. It should be noted that Eq. (9) is a modification of the equation presented by Marston et al. [26] and Atkins [27]. The matrix toughness has been replaced by the toughness of unreinforced syntactic foam containing 30 vol% phenolic microspheres, to account for the presence of the microspheres.

Values for the toughness contributions for SFRSF containing various amounts of short fibers are shown in Table 1 while Fig. 8b shows the conjectural estimate of Eq. (10). It is clear from Fig. 8b that the trend for the experimentally measured critical energy release rate vs. weight fraction of SCF is

Table 1
Estimated toughness contributions from individual toughening mechanisms: (i) interfacial debonding, R_d; (ii) strain redistribution energy, R_r; (iii) fiber pull-out, R_{po}, and (iv) formation of new surfaces, R_s

SCF weight fraction (wt%)	Equivalent volume fraction (vol%)	R_d (kJ/m^2)	R_r (kJ/m^2)	R_{po} (kJ/m^2)	R_s (kJ/m^2)	R_t (kJ/m^2)
0	0	NA	NA	NA	0.736 (100%)	0.736
1	0.48	0.0006 (~0.07%)	0.0082 (~0.96%)	0.0122 (~1.43%)	0.8334 (~97.54%)	0.8544
2	0.97	0.0012 (~0.12%)	0.0164 (~1.68%)	0.0245 (~2.52%)	0.9319 (~95.68%)	0.9740
3	1.46	0.0019 (~0.17%)	0.0247 (~2.26%)	0.0370 (~3.38%)	1.0313 (~94.19%)	1.0949

The relative percent from each contribution is indicated by the bracketed value.

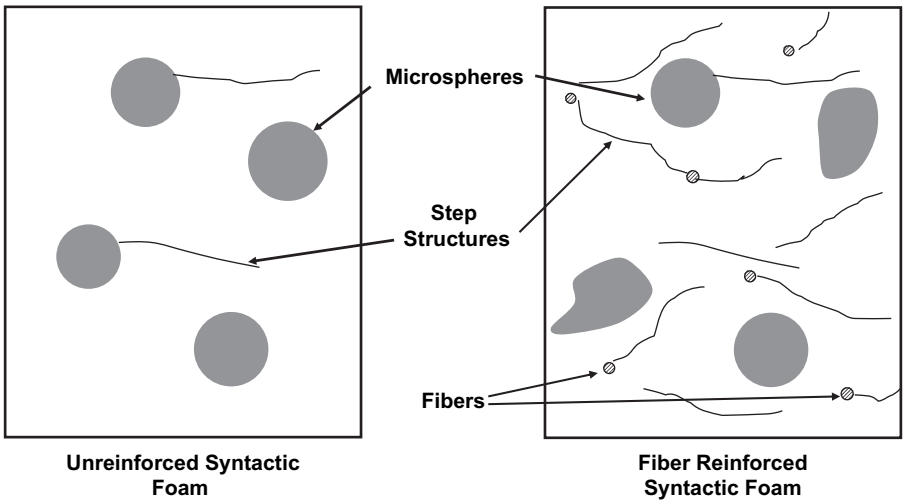

Fig. 11. Schematic of proposed fracture mechanisms of short fiber reinforced syntactic foam based on post-mortem observation using SEM.

consistent with the estimated values from Eq. (10). Although the values in Table 1 are based on SFRSF containing 3 mm fibers, similar values are expected for SFRSF containing fibers length of 4.5 and 10 mm since the fracture toughness of SFRSF is independent of the fiber length. From Table 1, it is clear that the formation of new surfaces due to fiber-assisted plasticity is the main contributor to the overall toughness of SFRSF. Formation of surfaces encompasses the formation of new matrix, fiber and microsphere surfaces. It has been reported [13] that the role of fiber and of other rigid phase additions such as the microsphere in a polymer matrix could be understood in the framework of a competing influence of enhanced plasticity and enhanced damage. In the composite, the strength of the fiber/matrix interface is crucial in influencing the overall balance between these competing processes. A stronger interface favors fiber-assisted localized plasticity whereas a weaker interface favors fiber-induced damage. Figs. 5 and 10a demonstrate a rather strong carbon fiber/epoxy interface. This interface appears considerably stronger than that observed for the microsphere/epoxy. It is clear that fiber reinforcement imparts additional step structures onto the fracture surface. These step structures are formed due to enhanced matrix plasticity [13]. They are considered as new surfaces that consume fracture energy. In addition to increased frequency, the step structures behind the broken fibers appear to be more intense compared to step structures observed behind microspheres. The increased roughness and frequency of the step structures indicate increased fracture energy for SFRSF compared to unreinforced syntactic foam. In addition to creating new fracture surfaces, it is observed that microspheres in the surroundings of the fibers show increased signs of debonding, see Fig. 10. The debonding of microsphere creates new microspheric surfaces and thus contributes to the additional toughening arising from hybrid interactive effects. It can thus be clearly demonstrated that the role of the fibers in increasing the composite fracture toughness is via creation of extensive step structures, debonding and fracturing of microspheres. An increase in the fiber loading will lead to an increase in stress field overlapping between fibers and microspheres, resulting in enhanced plasticity and a higher number of step structures and more severe debonding and fracturing of microspheres, leading to an increase in the fracture toughness.

Fig. 11 shows a schematic that summarizes our proposed fracture mechanisms of the fiber reinforced syntactic foam. The schematic illustrates the role of fiber-assisted plasticity that leads to more extensive step structures in the vicinity of carbon fibers as crack faces pass through. Fiber-assisted plasticity via formation of additional fracture surfaces appears to play a crucial role in the increase in overall toughness of the studied composites.

4. Conclusions

Based on the results presented in this paper, concomitant strengthening and toughening can be accomplished using carbon fiber reinforced syntactic foam, 3 wt% fiber reinforcement increased the tensile strength, Young's modulus, plane strain fracture toughness by 40, 115 and 95%, respectively. Such property improvements are considered impressive in polymer composites. The improvement in properties is caused by the synergistic interactions of short carbon fibers with microballoons in an epoxy matrix. Fiber-assisted plasticity introduces additional step structures, debonding and fracturing of microspheres from the matrix. As a result, new fracture surfaces that consume energy are created. The variation in fiber length between 3 and 10 mm does not affect the tensile and fracture properties significantly. A simple estimate based on the well-known Kelly–Tyson model indicates that the studied fiber lengths could plausibly exceed the critical fiber transfer length, l_c. The fiber content and fiber length do not affect the thermal properties of SFRSF. A conjectural estimate of the total fracture toughness gives rise to a similar trend to the measured fracture toughness of the composites studied.

Acknowledgements

The authors wish to thank Nanyang Technological University for the support of this work. One of us (EMW) would like to thank Ms. Lin Yiting for her contributions in processing and testing of the samples. SCW acknowledges the support of NSF MRI Grant# DMI 0520967 administered by the Design, Manufacturing and Innovation Division. The assistance provided by Ms. Shiyue Qu in the preparation of this manuscript at The University of Akron is also greatly appreciated.

References

[1] Bunn P, Mottram JT. Composites 1993;24:565.
[2] Rizzi E, Papa E, Corigliano A. Int J Solids Struct 2000;37:5773.
[3] Gupta N, Kishore K, Woldesenbet E, Sankaran S. J Mater Sci 2001; 36:4485.
[4] Huang Q, Kloetzer R, Seibig B, Paul D. J Appl Polym Sci 1998;69:1753.
[5] Ghazali Z, Johnson AF, Dahlan KZ. Radiat Phys Chem 1999;55:73.
[6] Karthikeyan CS, Sankaran S, Jagdish Kumar MN, Kishore K. J Appl Polym Sci 2001;81:405.
[7] Gupta N, Maharsia R. Appl Comp Mater 2005;12:247.
[8] Wouterson EM, Boey FYC, Hu X, Wong S-C. Comp Sci Technol 2005; 65:1840.
[9] Wouterson EM, Boey FYC, Chen L, Wong S-C, Hu X. Comp Sci Technol 2007, in press.
[10] Shutov FA. Syntactic polymer foams. In: Klempner D, Frisch KC, editors. Handbook of polymeric foams and foam technology. Hanser Publishers; 1991. p. 355.
[11] Friedrich K. Comp Sci Technol 1985;22:43.
[12] Wong S-C, Sui GX, Yue CY. J Mater Sci 2002;37:2659.
[13] Nair SV, Wong S-C, Goettler LA. J Mater Sci 1997;32(20):5335.
[14] http://rsb.info.nih.gov/ij.
[15] Norman DA, Robertson RE. J Appl Polym Sci 2003;90:2740.
[16] Lee J, Yee AF. Polymer 2000;41:8363.
[17] Hertzberg RW. Deformation and fracture mechanics of engineering materials. New York: Wiley; 1989. p. 337.
[18] Lauke B, Fu S-Y. Comp Sci Technol 1999;59:699.
[19] Fu S-Y, Lauke B. Comp Sci Technol 1996;56:1179.
[20] Chen C-H, Cheng C-H. Int J Solids Struct 1996;17:2519.
[21] Kelly A, Tyson WR. J Mech Phys Solids 1965;13:329.
[22] Kim JK, Mai YW. Engineered interfaces in fiber reinforced composites. Amsterdam, The Netherlands: Elsevier; 1998. p. 241.
[23] Lee J, Yee AF. Polymer 2001;42:577.
[24] Lee J, Yee AF. Polymer 2001;42:589.
[25] Lange FF. Philos Mag 1970;22:983.
[26] Marston TU, Atkins AG, Felbeck DK. J Mater Sci 1974;9:447.
[27] Atkins AG. J Mater Sci 1975;10:819.